Journal of Research and Applications in Mechanical Engineering
ISSN: 2229-2152 (Print); 2697-424x (Online)
(2025) Vol. 13, No. 3, Paper No. JRAME 25-13-046
[DOI: 10.14456/ jrame.2025.46]

*Research Article*

# Improvement of Spatial Resolution of W-BOS Analysis Images in Supersonic Flow Using Super-Resolution Technique

**K. Maeda**
**H. Fukuoka***
**A. Suda**
**Y. Taniguchi**
**K. Hiro**
**S. Nakamura**
*National Institute of Technology (KOSEN), Nara College, Yamatokoriyama 639-1080, Japan*

**Received** 6 September 2024
**Revised** 24 January 2025
**Accepted** 27 January 2025

**Abstract:**
*The Wavelet-based Background Oriented Schlieren (W-BOS) method quantitatively evaluates the density gradient. This study achieves high spatial and temporal resolution in the density gradient images by integrating a super-resolution technique and the W-BOS method. This experiment uses a jet and a jet-induced shock wave emitted from an open small-volume shock tube as visualization targets. We investigated the effect of super-resolution model types and restoration magnification ratios. Three established super-resolution models are used to restore. The magnifications of 2, 4 and 8 are evaluated. At magnifications 2 and 4, the processed images were close to the original, with the shock wave and the jet well captured in all super-resolution models. In the restoration of magnification 4 using the EDSR model, a measurement error was about 15% smaller than a Bicubic interpolation. These results suggest that the W-BOS method is capable of super-resolution restoration of high-resolution images with magnifications up to 4.*

**Keywords:** *Supersonic Flow, Shock Wave, Background Oriented Schlieren, Wavelet Transformation, Super-Resolution*

## 1. Introduction

The Background Oriented Schlieren (BOS) method is a visualization technique proposed by Meier [1] and Dalziel [2] that enables quantitative evaluation of a density gradient of flow fields. The BOS method uses the refraction of light caused by density changes in the flow fields to obtain the density gradient from the difference between a measurement image with flow and a reference image without flow. The Wavelet-based BOS (W-BOS) method proposed by Akatsuka et al. [3] is based on the BOS method. It applies a continuous wavelet transform to a sinusoidal background image to calculate a quantitative density gradient image from the phase difference. As studies similar to the W-BOS method, a report on improving the BOS method focuses on the amplitude of the wavelet transform [4]. Additionally, the visualization of convective heat transfer using the phase obtained by continuous wavelet transform has been explored [5]. Another study utilizes a two-dimensional sine wave as a background image [6], while a different approach employs a Fourier transform for a sinusoidal waveform background image [7]. The W-BOS method has been shown to produce the density gradient image as clearly as the Schlieren method.

In the visualization of supersonic flows, high-speed imaging using a high-speed camera involves a trade-off between frame rates and image resolutions. In the W-BOS method, the measurement accuracy of the phase difference corresponding to the density gradient depends on the image resolution. In other words, in the W-BOS method, it is desirable to improve the image resolution to visualize local density gradient changes in supersonic flows.

Studies using super-resolution techniques in visualization techniques using high-speed cameras have been reported in recent years. The super-resolution technique is an image processing technique that generates a high-resolution

* Corresponding author: H. Fukuoka
E-mail address: fukuoka@mech.nara-k.ac.jp

image by interpolating unknown pixels from a low-resolution image. For example, studies have been reported using the super-resolution technique in supersonic flow fields to recover a high-resolution Schlieren image [8][9][10]. Katsunari Ota et al. [11] also reported a study using the super-resolution technique based on neural networks to improve the spatial resolution of visualized images using the BOS method.

The BOS method is characterized by its relatively simple imaging system consisting of a background image, a light source, and a camera, compared to the Schlieren method, which uses lenses and knife edges in its optical system to detect light refraction. However, the spatial resolution of the BOS method is low. Therefore, we focused on the super-resolution technique, which is a technique to increase the spatial resolution of low-resolution images. Experimental images in the W-BOS method are composed of sinusoidal periodic data, which is considered to have a high affinity for the super-resolution technique. However, the results of applying the super-resolution technique to the W-BOS method are unclear. This study aims to improve the spatial resolution in supersonic flows by applying the super-resolution technique to the W-BOS method. This experiment uses the jet and the jet-induced shock wave emitted from an open small-volume shock tube as visualization targets. The accuracy of the super-resolution reconstruction is quantitatively evaluated by comparing the experimentally captured images with images reconstructed using super-resolution on a pre-scaled image. If the super-resolution technique increases the resolution of analytical images obtained by the W-BOS method, it will be possible to capture detailed density changes during the passage of jets and shock waves. These are expected to be applied to the visualization of supersonic phenomena.

## 2. Principle of BOS Method

Figure 1 shows an overview of the BOS method's optical apparatus and measurement principle. The optical system mainly consists of a background image, a camera, and a light source. The solid and dashed lines in Fig. 1 show the path of light traveling from the background image in the absence and presence of a density gradient, respectively. The light from the background image is refracted by the density gradient, as shown by the dashed line. The camera receives the refracted light with a shift of $\Delta h$ compared to the case where the straight line indicates no density gradient. The refractive index gradient in the density change region is expressed by Equation (1).

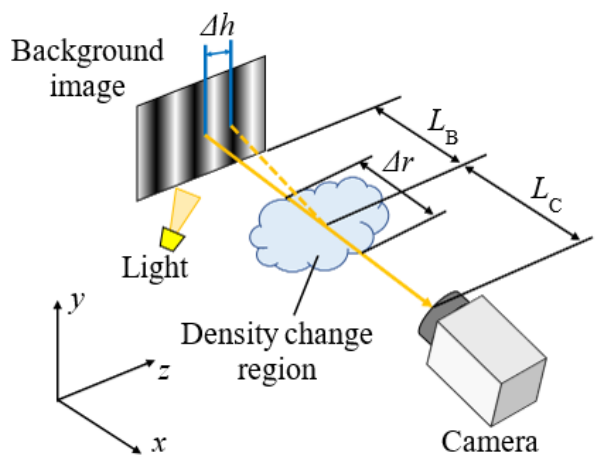


**Fig. 1.** Optical device for BOS method.

$$\int_0^{\Delta r} \frac{\partial n}{\partial z} dx = n_0 \frac{\Delta h}{L_B - \Delta r/2} \tag{1}$$

In equation (1), $\partial n/\partial z$, $n_0$, $L_B$, and $\Delta r$ are the refractive index gradient in the density change region, the refractive index of air, the distance between the background image and the density change region and the width of the density change region, respectively. In this study, $n_0 = 1.00027$ because the experiment is conducted at an air temperature of 20 °C. The relationship between the refractive index and density is expressed by Equation (2).

$$n = G\rho + 1 \tag{2}$$

$n$, $G$, and $\rho$ in equation (2) are the refractive index, Gladstone-Dale constant, and air density, respectively. In this study, $G = 2.3156\times10^{-4}$ m$^3$/kg. From equations (1) and (2), quantitatively, it is possible to determine the density gradient in the z-direction.

## 3. Experimental and Super-Resolution Methods

### *3.1 Visualization method*

In the W-BOS method, the difference between the measurement and the reference images is calculated by continuous wavelet analysis to obtain the phase difference between the respective luminance distributions. Using this phase difference, the density gradient is calculated by applying the Gladston-Dale Relation, which relates density to the refractive index. Since this method yields a quantitative density gradient distribution, it is possible to calculate the density distribution by integrating it. The detailed principle and analysis method for the W-BOS method are described in our previous paper [4]. In this study, in addition to the conventional method described above, the super-resolution technique is applied to the measurement and the reference images, and continuous wavelet analysis is performed after interpolating pixels. Experimental images in the W-BOS method are compatible with super-resolution techniques because they consist of sinusoidal data. Thus, the experimental image is used as the object of restoration by the super-resolution technique instead of the processed image.

Figure 2 shows an overall view of the experimental apparatus. The experimental apparatus consists of a shock tube, high-pressure air cylinder, regulator, valve, pressure sensor, and visualization system. A pressure sensor measures the pressure in the high-pressure chamber of the shock tube. The shock wave and the jet are generated by rupturing the diaphragm with a striker pin when the pressure in the high-pressure chamber reaches a predetermined pressure. The pressure ratio between the high-pressure chamber and the low-pressure chamber (atmospheric pressure) in the shock tube was set to 35.0. The velocity of the jet, the shock Mach number, and the pressure ratio across the shock wave are approximately 210 m/s, 1.21, and 1.53, respectively, generated in the experiment with the pressure ratio of 35.0 in the shock tube.

The visualization system for the W-BOS method consists of a background image, LED light source (nac's LLBK1-LA-W-0001 high-brightness LED lighting equipment), and a high-speed camera (nac's HX-3 high-speed camera). The high-speed camera had an image size of 1280 × 736 pixels, a shooting speed of 10000 fps, an exposure time of 10 μs, and an $F$ value of 5.6. In Fig. 2, $L_B$ and $L_C$ are the distance between the background image and the density change area, as well as between the shock tube center and the high-speed camera. $L_B$ and $L_C$ are 200 mm and 2500 mm, respectively. The background image is a sinusoidal vertical stripe pattern with a period of 2 mm.

The phase difference between the measurement and the reference images was calculated using continuous wavelet analysis, a time-frequency analysis technique. Continuous wavelet analysis is a method of analyzing signals that employ basis functions, known as mother wavelets, to facilitate the scaling, translation, and transformation of the signal across the time axis. The mother wavelet in the wavelet transform is the Gabor complex wavelet function.

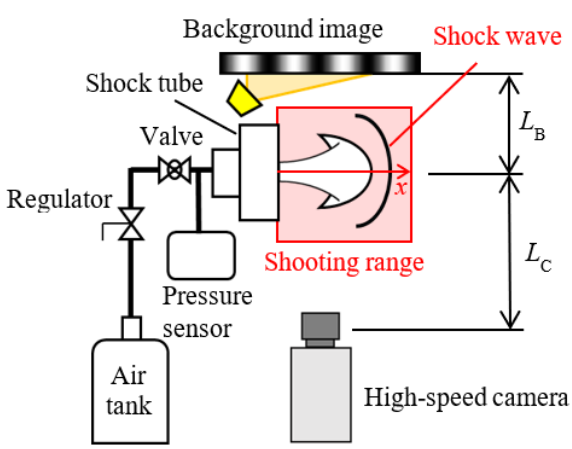


**Fig. 2.** Experimental apparatus.

*3.2 Evaluation method for restoration with super-resolution*

This section describes a method for quantitatively evaluating the accuracy of the super-resolution restoration in the W-BOS method. Figure 3 illustrates the evaluation procedure for the super-resolution restoration. Fig. 3 (a)-(c) shows a high-resolution image (HRI) taken in the experiment, a low-resolution image (LRI) obtained by reducing the high-resolution image, and a super-resolution image (SRI) obtained by restoring the low-resolution image, respectively. Thus, the HRI is reduced using the Bicubic method, an interpolation method that uses information from 16 pixels around a pixel. Super-resolution models and the Bicubic method were used to restore the LRI. The super-resolution models include the Efficient Sub-pixel Convolutional Neural Network (ESPCN), the Fast Super-Resolution Convolutional Neural Network (FSRCNN), and the Enhanced Deep Super-Resolution Network (EDSR), which are single image super-resolution methods. The super-resolution models were the pre-trained models provided by the OpenCV library in Python. Each of the provided trained models is trained on the DIV2K dataset, which consists of 2K-resolution images used in research on super-resolution techniques. In this paper, we investigate the effect of the super-resolution restoration magnification ratio on the luminance distribution and the sharpness of the density gradient images. The high-resolution images taken in the experiment are reduced to 1/2, 1/4, and 1/8 and restored to their original size at the magnification ratios of 2, 4, and 8, respectively.

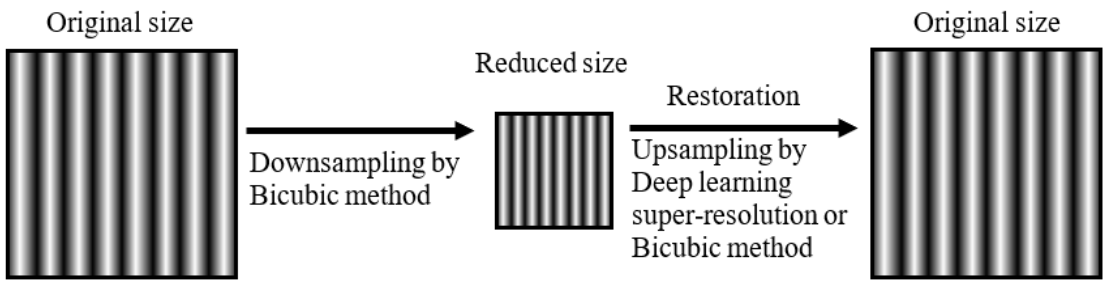


(a) HRI (b) LRI (c) SRI

**Fig. 3.** Evaluation procedure for restoration with super-resolution. (a) HRI: high-resolution image, (b) LRI: low-resolution image and (c) SRI: super-resolution image

To evaluate the sharpness of the density gradient images, the Root Mean Square Error (RMSE) was used. The RMSE is calculated by Equation (3), where $N$ is the total number of pixels in the high-resolution. $y_i$ and $\hat{y}_i$ are the density gradient calculated by the W-BOS method in the high-resolution image and the density gradient in the super-resolution image, respectively.

$$\mathrm{RMSE} = \sqrt{\frac{1}{N}\sum_{i=1}^{N}(y_i - \hat{y}_i)^2} \tag{4}$$

**4. Results and Discussion**

*4.1 Effect of restoration magnification ratio on the accuracy of restoration*

In this section, we evaluate the accuracy of the image restoration by changing the magnification ratio of the image restored by the super-resolution model to investigate the effectiveness of the image restoration by super-resolution for the experimental images before continuous wavelet analysis. Figure 4 shows the HRI and the super-resolution image (SRI) restored from the LRI by EDSR. In Fig. 4, the vertical stripe pattern indicates the sinusoidal distribution with a period of 2 mm. The evaluation images were taken from experimental images of transient flow at the pressure ratio of 35.0 and $t$ = 200 μs. The time $t$ is set to 0 s, one frame before the jet is ejected from the shock tube. The 2SRI, 4SRI, and 8SRI images in Fig. 4 are experimental images restored at the magnification ratios of 2, 4, and 8, respectively. Fig. 4(a) shows that the vertical stripes in the background image are distorted in the horizontal direction at $x/D$ = 2 - 4. This is due to the refraction of the light by the density gradient of the jet ejected from the shock tube. In the 2SRI and 4SRI images shown in Fig. 4(b) and 3(c), optical distortion can be observed at $x/D$ = 2 - 4, as in the HRI image. In the 8SRI shown in (d), the width of the shading is narrower throughout the image, and the gray areas are larger.

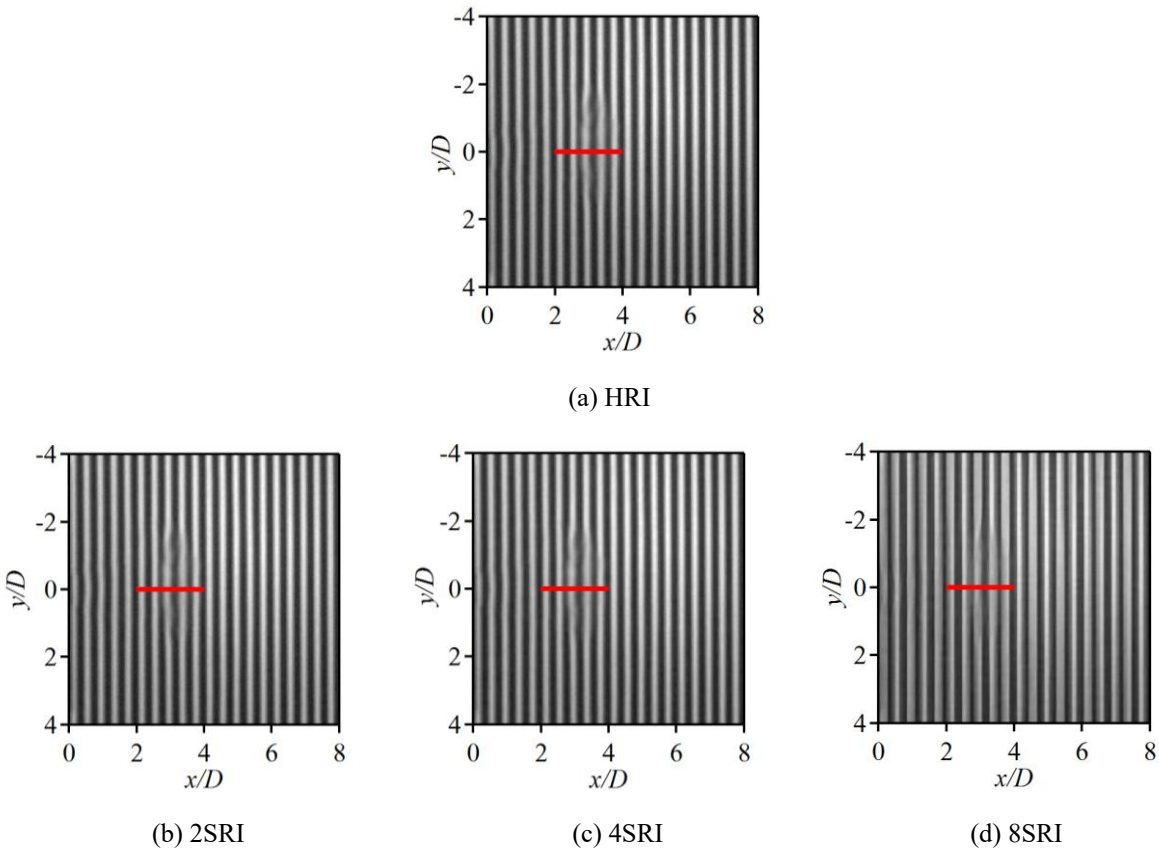


(a) HRI

(b) 2SRI (c) 4SRI (d) 8SRI

**Fig. 4.** Comparison between HRI and SRI restored for the magnification ratios of 2, 4, and 8 in EDSR.

From the above, we have confirmed that the super-resolution method can be used to qualitatively restore the experimental image before continuous wavelet analysis up to the magnification ratios of 2 and 4. To quantitatively compare the accuracy of pixel interpolation using the super-resolution method, we focus on the luminance distribution in the highly distorted region on the red line shown in Fig. 4(a). Figure 5 shows the luminance distribution along the central axis of the shock tube ($y/D$ = 0, $x/D$ = 2 - 4) in Fig. 4(a) - (d). The number of pixels in the luminance distributions shown in Fig. 5 is about 70 pixels per $x/D$. Fig. 5 shows that the luminance distributions of 2SRI and 4SRI almost reproduce the HRI waveforms, while the luminance distribution of 8SRI has a larger difference in amplitude and phase than that of HRI. Therefore, it is clear that the performance of the low-resolution image restoration using the super-resolution method is lower at the magnification ratio of 8.

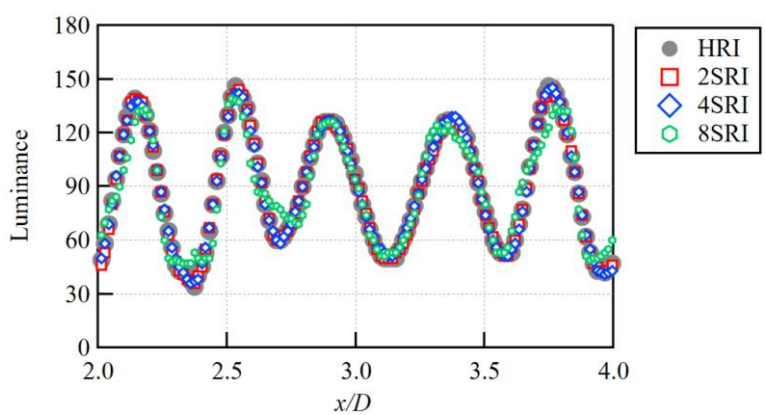


**Fig. 5.** Comparison of luminance distribution between HRI and SRI restored for magnification ratios of 2, 4, and 8 in EDSR.

*4.2 Effect of super-resolution restoration on the density gradient image*

The previous section clearly shows that the experimental image restoration using the super-resolution technique has highly accurate at the magnification ratios of 2 and 4. Next, to investigate the effect of the experimental image restoration by super-resolution on image processing using continuous wavelet analysis, we focus on the density gradient image after image processing. Figure 6(a)-(d) show the density gradient images corresponding to Fig. 4(a)-(d). In the HRI of Fig. 6, the jet head and the shock wave can be observed at $x/D$ = 3.8 and $x/D$ = 5.5 at $y/D$ = 0, respectively. The jet and the shock wave in the 2SRI and the 4SRI are almost identical to those of the HRI. In the case of the 8SRI, the jet outlines at $x/D$ = 0 - 4 are blurred compared to the HRI. The 2SRI and 4SRI images clearly show the jet and the shock wave. This is because the sinusoidal luminance distribution was reproduced in the reconstruction of the experimental images at magnification ratios of 2 and 4 using the super-resolution method.

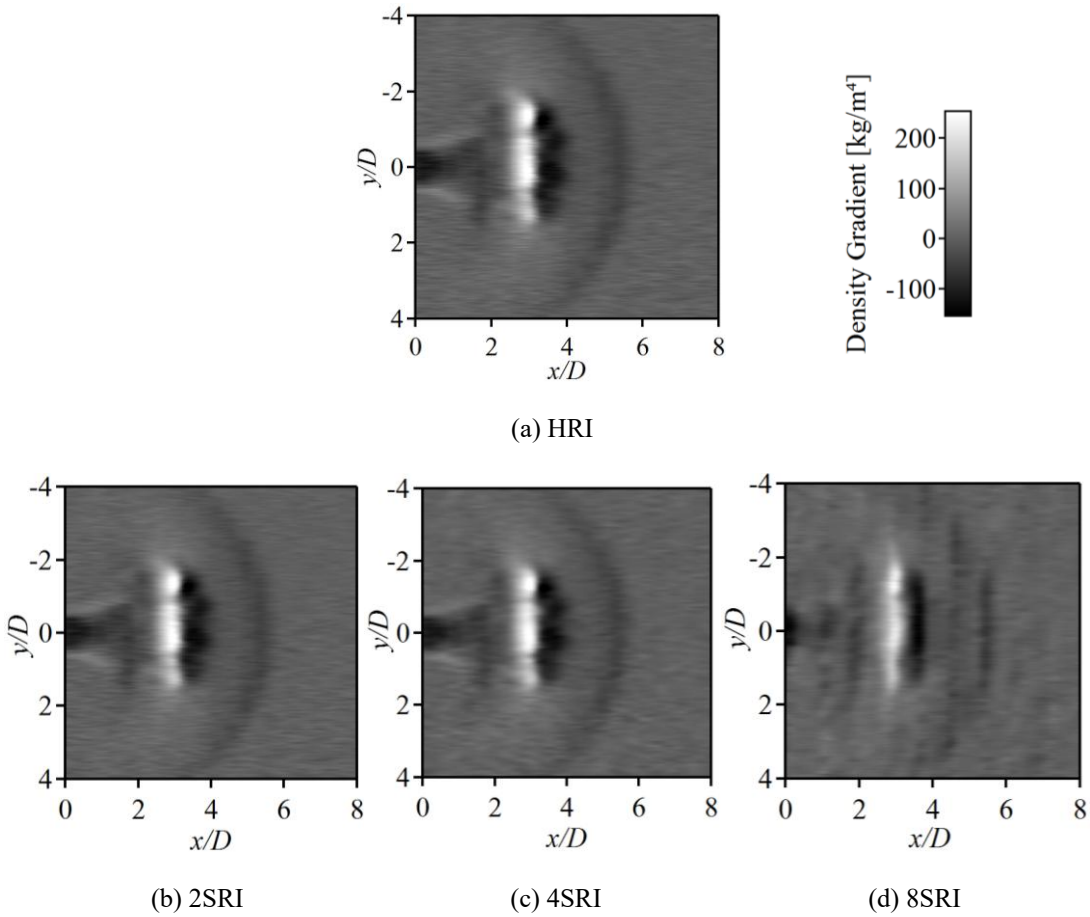


(a) HRI

(b) 2SRI (c) 4SRI (d) 8SRI

**Fig. 6.** Comparison of density gradient images between HRI and SRI restored for magnification ratios of 2, 4, and 8 in EDSR.

To identify the super-resolution model compatible with the continuous wavelet analysis in the W-BOS method, it is necessary to evaluate the accuracy of the restoration using multiple super-resolution models. Figure 7 shows the RMSE change restoring multiple super-resolution models at different magnification ratios. The RMSE is the root mean square error of the density gradients that comprise the HRI and SRI in Fig. 7. Fig. 7 shows that the RMSE increases as the magnification increases from the magnification ratios of 2 to 8 for three models. This indicates that the HRI becomes more difficult to reproduce at higher magnifications for all super-resolution models and Bicubic interpolation. At the lowest magnification ratio of 2, there is little difference in RMSE among the different super-resolution models. At the magnification ratio of 4, the RMSE is the lowest with EDSR and the highest with the Bicubic method. Thus, at this magnification ratio, trained super-resolution methods such as EDSR performed better than the Bicubic method, a mathematical interpolation method. At the magnification ratio of 8, the model with the

lowest RMSE was the FSRCNN. However, the processed image was as blurred as that of EDSR. Thus, the optimal super-resolution model could not be identified at the higher restoration magnification ratio of 8. Based on the above results, the best-performing super-resolution model for the W-BOS method is EDSR, which is effective for image restoration up to the magnification ratio of 4 in cases where the super-resolution method is applied. To further improve restoration accuracy using the super-resolution models, it is considered necessary to train experimental images.

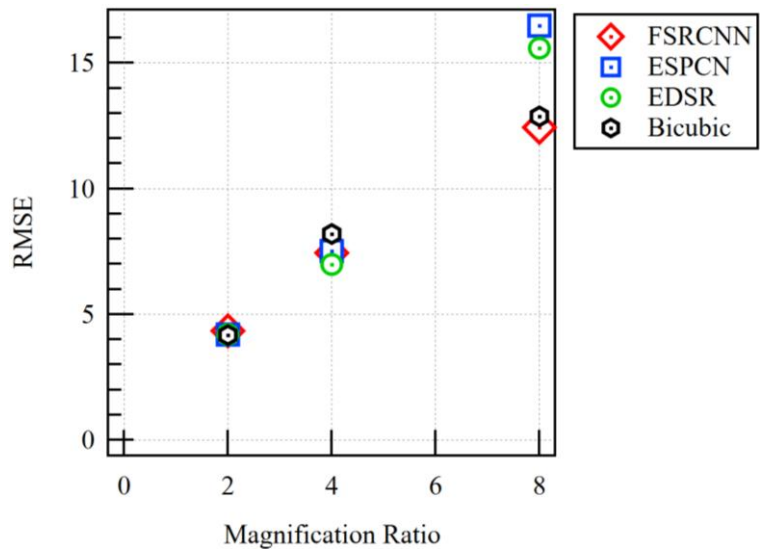


**Fig. 7.** Relationship between magnification ratio and RMSE of density gradient for three models.

## 5. Conclusion

In this study, we aimed to improve the spatial resolution of W-BOS analysis images in the supersonic flow using super-resolution techniques. This paper's visualization targets are the jet and the jet-induced shock wave emitted from the small-volume shock tube. To investigate the effectiveness of super-resolution techniques in the W-BOS method, the comparison was made between the high-resolution image and the image of the same size restored by the super-resolution models. The super-resolution restoration magnification ratio was changed to 2, 4, and 8 as parameters. The image processing results by continuous wavelet analysis on the restored image using the super-resolution models showed that the density gradient images were qualitatively similar to the high-resolution image at the magnification ratios of 2 and 4. The reconstruction at a larger magnification ratio of 8 was found to be fundamentally difficult due to the blurring of the jet and the shock wave using all models. The results show that the super-resolution models effectively restore images up to the magnification ratio of 4 in the W-BOS method. The EDSR model was the most accurate restoration at the magnification ratio of 4, suggesting that it is the best of the three super-resolution models used in this study. These results suggest that applying super-resolution techniques to the experimental images before image processing improves the spatial resolution of the density gradient images.

## References

[1] Meier G. Computerized background-oriented schlieren. Experiments in Fluids. 2002;33:181-187.
[2] Dalziel S, Hughes G, Sutherland B. Whole-field density measurements by ‘synthetic schlieren’. Experiments in Fluids. 2000;28(4):322-335.
[3] Akatsuka J, Nagai S, Honami S. Improved Flow Visualization Methods Based on the Background Oriented Schlieren Technique. Transactions of the Japan Society of Mechanical Engineers. 2011;77(784):2391-2400.
[4] Miyaoku K, Fukuoka H, Nakamura S, Yao M, Hiro K. Improvement of Background Oriented Schlieren Method Focused on Amplitude of Wavelet Transform. IOP Conf. Series: Materials Science and Engineering. 2019;886(012037):1-8.
[5] Rajshekhar G, Ambrosini D. Multi-scale approach for analyzing convective heat transfer flow in background-oriented Schlieren technique. Optics and Lasers in Engineering. 2018;110:415-419.

[6] Schmidt B, Woike M. Wavelet-Based Optical Flow Analysis for Background-Oriented Schlieren Image Processing. AIAA Journal. 2021;59(8):1-20.
[7] Ramaiah J, Rubeis T, Gannavarpu R, Ambrosini D. Quantitative flow visualization by hidden grid background oriented schlieren. Optics and Lasers in Engineering. 2023;160(107307):1-7.
[8] Kong C, Chang J, Wang Z, Li Y, Bao W. Data-driven super-resolution reconstruction of supersonic flow field by convolutional neural networks. AIP Advances. 2021;11(6):1-14.
[9] Ekwonu M, Zhang S, Chen B. Super-resolution reconstruction of schlieren images of supersonic free jets based on machine learning with bubble shadowgraphy data. Journal of Visualization. 2023;26:1085-1099.
[10] Wang Z, Li X, Liu L, Wu X, Hao P, Zhang X, He F. Deep-learning-based super-resolution reconstruction of high-speed imaging in fluids. Physics of Fluids. 2022;34(3):1-22.
[11] Ota K, Ukai T, Wakai T. Spatial resolution improvement by a super-resolution technique depending on training process in the background-orientated schlieren analyses. Physics of Fluids. 2023;35(12):1-11.